Journal of Sound and Vibration (2002) **249**(4), 701–718
doi:10.1006/jsvi.2001.3836, available online at http://www.idealibrary.com on IDEAL®

NON-LINEAR VIBRATION ABSORBER FOR A SYSTEM UNDER SINUSOIDAL AND RANDOM EXCITATION: EXPERIMENTS

O. Cuvalci

WCVD Product Unit, Applied Materials, Santa Clara, CA 95054, *U.S.A.*

A. Ertas and S. Ekwaro-Osire

Department of Mechanical Engineering, Texas Tech University, Lubbock TX 79409, *U.S.A.*

and

I. Cicek

Faculty of Marine Engineering, Istanbul Technical University, Istanbul, Turkey

(*Received* 8 *January* 2001, *and in final form* 11 *May* 2001)

A system consisting of a primary structure coupled with a passive tuned vibration absorber is experimentally studied. The primary structure consists of four flexible columns with a mass, while the absorber consists of a beam with a tip-mass. The system, which is a coupled non-linear oscillator, is subjected to sinusoidal and random excitation. The effects of the forcing frequency, forcing amplitude, mass ratios and frequency ratios on the displacement response of the system in the neighborhood of the autoparametric region are studied. Control parameters related to effectiveness of the absorber are determined. The objective of this study is to experimentally define an absorption region for the passive vibration absorber and to determine the parameters that influence the effectiveness of the vibration absorber.

1. INTRODUCTION

Mitigation or attenuation of vibrations is essential in most engineering equipment, particularly, where high-amplitude oscillations could lead to the malfunction of essential system components or the damage of sensitive payloads. Vibration mitigation has found extensive usage in aerospace structures, civil engineering structures, and mechanical machinery. Recently, a comprehensive survey on vibration suppression devices was given by Sun *et al.* [1]. They reviewed the current developments in passive absorbers, adaptive absorbers, and active absorbers. Passive tuned vibration absorbers are among the most widely used classical vibration absorbers. Passive tuned vibration absorbers are also referred to as dynamic vibration absorbers [2] or tuned mass dampers [3].

Watts [4] performed one of the earliest studies on a dynamic vibration absorber. He presented his study in the context of mitigating the rolling of ships at sea. A mathematical model of a passive dynamic vibration absorber was investigated by Ormondroyd and Hartog [5]. Most vibration absorption devices have been studied with systems under sinusoidal excitation. While studying the optimal use of a mass in a vibration absorber,

0022-460X/02/040701 + 18 $35.00/0

Dahlberg [6] clearly showed that continuous absorber is more effective than a mass–spring–damper absorber. Recently, Kawazoe *et al.* [7] performed detailed numerical studies on a beam-type vibration absorber. By investigating the response of the beam-type absorber in conjunction with the response of the system, they demonstrated the effectiveness of this kind of vibration absorber. Liquid vibration absorbers have also found practical use in civil engineering constructions and in satellite technology. All the previously mentioned engineering structures have generally low natural frequencies. Hitchcock *et al.* [8] presented characteristics of a liquid column vibration absorber as they relate to applications on tall buildings. They also presented techniques that could be used to control and predict absorber characteristics. Modi and Seto [9] carried out extensive experimental study on the control of wind-induced vibrations using liquid vibration absorber. They studied how the absorber parameters, specifically, geometry and liquid content, affected its performance. There have been numerous studies on vibration absorbers for systems under random excitation. Wirsching and Campbell [10] studied the structural response of a linear multi-story building having a linear vibration absorber attached to the roof under random excitation. They demonstrated that the absorber was quite effective in reducing first mode response for 5 and 10 story structures even with relatively small values of the absorber mass.

An effective vibration absorber extracts oscillatory energy from the primary structure. This kind of energy transfer is well demonstrated in autoparametric vibration. Autoparametric vibration exists when the conditions of internal resonance and external resonance are met simultaneously due to external force [11]. The basic feature of autoparametric resonance is the energy transfer when the lower mode frequency is equal to one-half of the higher mode frequency. Due to energy transfer, the lower mode may result in exponential energy growth and may act as a vibration absorber to the excited mode (higher mode). Autoparametric vibration can also be viewed as a special case of parametric vibration that refers to oscillatory motion resulting from time-dependent excitations. Parametric vibration is characterized by time-dependent coefficients of inertia, damping or stiffness terms in the governing differential equations. Small parametric excitations can produce a large response if the frequency of the excitation is closer to one of the natural frequencies of the system [12].

Autoparametric vibrations have been extensively studied for systems under sinusoidal excitations. Ibrahim and Barr [11] performed a theoretical and experimental study for two-mode interaction of a system under sinusoidal excitation. They showed that a weak coupling existed between the liquid sloshing and vertical motion of the primary structure. Sevin [13] numerically showed that for a pendulum-type absorber, a complete energy transfer could occur between two modes. It was shown that this phenomenon occurred when the beam frequency was twice that of the pendulum frequency. Non-linear vibration absorbers have also been recently investigated; particularly, as regards the conditions that impact the effectiveness of the absorber [14]. Numerous authors using the idea of mode interaction also studied different kinds of models involving autoparametric resonance [15–21]. For systems under random excitation, the autoparametric interaction has also been observed. Roberts [22] experimentally and theoretically studied a two-degree-of-freedom (d.o.f.) system, with quadratic non-linear coupling, under random excitation. His studies were focused on establishing stability boundaries for such systems with inherent autoparametric interaction.

In this paper, a primary structure, consisting of four flexible columns with a mass, M, and a passive tuned vibration absorber, consisting of a beam with a tip-mass, m, is experimentally investigated. Here, the vibration absorber coupled to the primary structure will be referred to as a system. In other literature, such a coupled system is also referred to as a composite system [1]. The experimental model used in this study is shown in Figure 1.

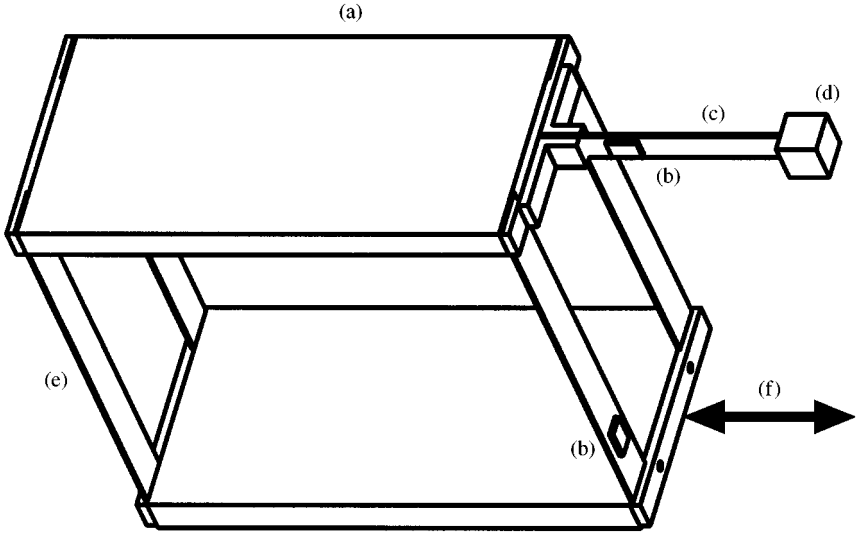

Figure 1. Experimental model of the system: (a) upper plate, (b) strain gages, (c) beam, (d) tip mass, (e) column and (f) excitation (sinusoidal and random).

This can be viewed as simulating a one-story building with a beam–mass-type vibration absorber. Ibrahim *et al.* [23] showed that the equations of motion of such a system are autoparametrically coupled. Hence, the system under study is a coupled non-linear oscillator. In the study presented here, a series of parametric experimental studies was performed to investigate the response of the non-linear dynamics of the system subjected to sinusoidal and random excitations. To study non-linear dynamics under autoparametric resonance conditions, the system was investigated in the neighborhood of its natural frequencies. The autoparametric condition is $\Omega = \omega_s = 2\omega_a$, where Ω, ω_s, and ω_a are the forcing frequency, the natural frequency of the system (higher mode), and the natural frequency of the absorber (lower mode) respectively. The primary objective of this study is to experimentally define an *absorption region* for the passive vibration absorber and to determine the parameters that influence the effectiveness of the vibration absorber.

2. EXPERIMENTAL SET-UP

The basic experimental apparatus used in this analysis is shown in Figure 2. The primary structure is a solid rectangular steel block supported by four steel spring beams 1·56 mm thick $\times$ 25·4 mm wide. The vibration absorber also consists of the same size steel spring beam with an adjustable end mass. The absorber system is attached to the main mass by a rigid clamp. The base of the model is restrained to horizontal motion by the use of four bearings moving on a smooth flat surface. The sinusoidal and random excitation was introduced horizontally to the base of the primary structure via a rigid attachment.

A vibration control system comprising a sweep generator (Trig-Tek Model 701LM), a signal compressor (Trig-Tek Model 801B), a vibration monitor (Trig-Tek Model 610B), and a multi-level programmer (Trig-Tek Model 831) generated the sinusoidal excitation signal. A random vibration equalizer analyzer (Trig-Tek Model 910B) generated the random excitation signal. A power amplifier (MB Dynamics Model S6K) amplified the generated signal. The amplified signal drove a 1200 lb electro-dynamic shaker

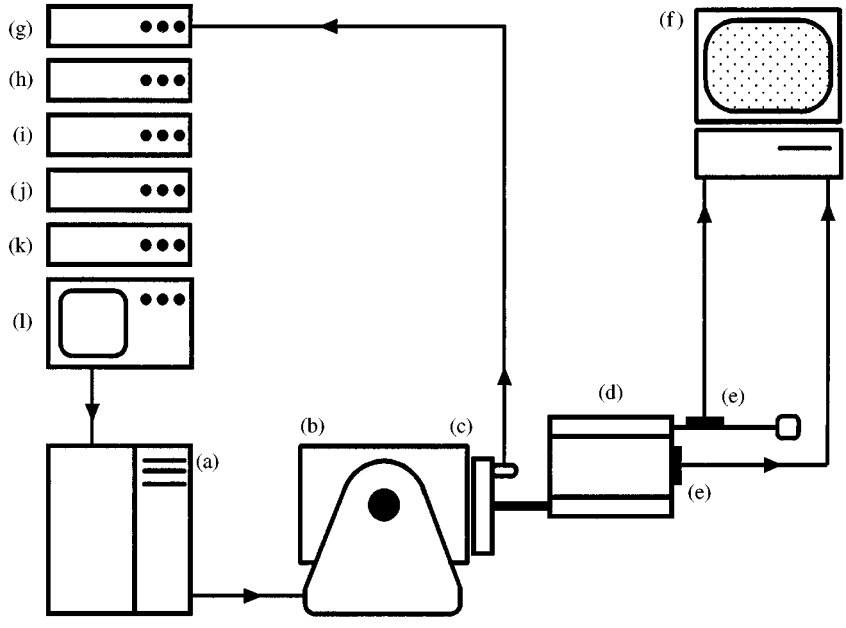

Figure 2. Experimental set-up: (a) power amplifier, (b) shaker, (c) accelerometer, (d) structural model, (e) strain gages, (f) computer and data acquisition, (g) vibration monitor, (h) compressor, (i) multi-level programming, (k) sweep generator and (l) random control system.

(MB Dynamics Model C10E). The data acquisition and processing system was made up of an Apple Macintosh IIfx computer with National Instruments NB-MIO-16X board, and LabView analysis and data acquisition software. During the experiments, the computer was used to store, display, and analyze experimental data. Additionally, for the sinusoidal excitation experiments, a four-channel digital storage and analysis system (Modal Data 6000) was used. It should be noted that both the sinusoidal and random signal generators also had feedback signals from the shaker to accomplish the signal control task.

Two strain gages (piezo films) were used as transducers to monitor the displacement response of the system and the vibration absorber (Figure 1). The first strain gage was attached to the beam element of the vibration absorber, while the second strain gage was attached to one of the beam elements of the primary structure. An accelerometer (PCB Quartz Compression ICP Model 353B04) was attached to the table of the shaker to monitor its motion. The signals from the two strain gages on the primary structure and absorber, and the accelerometer on the shaker were fed into the data acquisition and analysis system.

3. RESULTS AND DISCUSSION

3.1. SINUSOIDAL EXCITATION

To study the vibration mitigation of the system by the vibration absorber, the system was excited at frequencies closer to its natural frequency. This was achieved by monotonically varying (sweeping) the forcing frequency in a selected interval at the sweep rate of 0·01 Hz/s with a constant amplitude. This frequency-sweep approach is similar to that taken by Hitchcock *et al.* [8] to study a liquid column vibration absorber. For the current study,

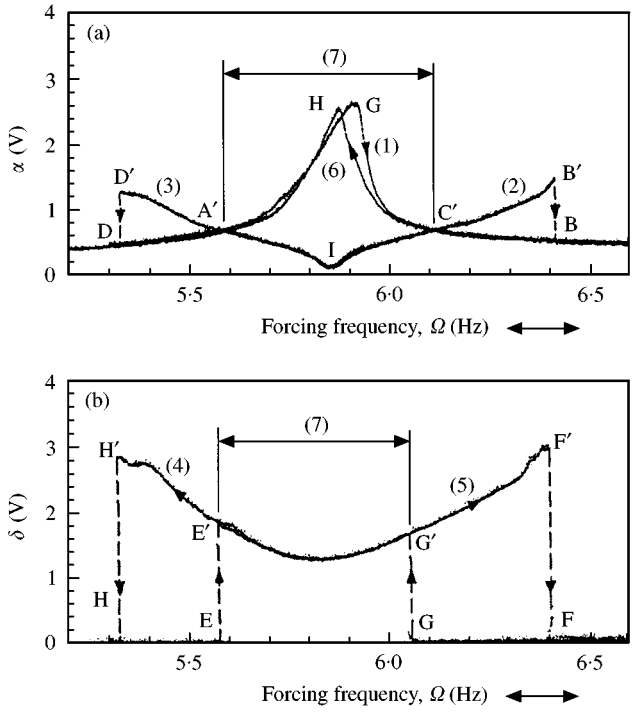

Figure 3. Experimental displacement response curves defining absorption region ($\omega_a = 0{\cdot}5\ \omega_s$): (a) system; (b) absorber. Response without activated absorber. System: (1) up sweep; (6) down sweep. Response with activated absorber. Up sweep: (2) system; (5) absorber. Down sweep: (3) system; (4) absorber. Jump points for up and down sweep. System: A′, B, B′, C′ D, and D′; absorber: E, E′, F, F′, G, G′, H and H′.

preliminary experiments were done to show that the sweep rate of 0·01 Hz/s was satisfactorily small to eliminate transient effects due to the change in forcing frequency. The effectiveness of the vibration absorber was studied by carrying out parametric studies on various parameters, namely, the forcing frequency, the forcing amplitude, the mass ratio of the absorber to primary structure, and the natural frequency ratio of the absorber to system (see Figure 1).

To effectively study the mitigation of vibrations, not only was the amplitude of the system monitored, but also that of the vibration absorber. To demarcate the *absorption region* for a selected frequency range, data were recorded for both the down sweep and up sweep of the frequency. The data were collected from the two strain gages located on the vibration absorber and the primary structure (see Figure 1). For the initial sets of experiments, the forcing amplitude, f, was set to 2·28 mm (peak-to-peak) and the natural frequency, ω_s, of the system was set to 5·78 Hz. This was achieved by attaching the absorber to the primary structure in a manner that resulted in the system having only one d.o.f. In this paper, the latter configuration will also be referred to as the case when the absorber is locked.

For the first set of experiments, the vibration absorber was tuned to yield the frequency relation $\omega_s = 2\omega_a$. This was achieved by simply adjusting the length of the beam of the vibration absorber. Additionally, the mass ratio of the absorber to primary structure, m/M, was adjusted to 0·086. The amplitudes of the system (with and without an activated absorber) and the vibration absorber were plotted against the corresponding frequencies. Figure 3 shows the characteristic responses of the system and the vibration absorber. It should be noted that Figure 3 show data from four distinct experiments: (1) forcing

frequency down sweep for the system with locked absorber; (2) forcing frequency up sweep for the system with locked absorber; (3) forcing frequency down sweep for the system with the activated absorber; and (4) forcing frequency up sweep for system with the activated absorber.

Each of the above experiments contained 2000 data points. The system displacement response is shown by curve 6 (data along BC′HA′D), for forcing frequency down sweep for the system with a locked absorber. The system displacement response is shown by curve 1 (data along DA′GC′B), for forcing frequency up sweep for the system with a locked absorber. The system displacement response is shown by curve 3 (data along BC′IA′D′D), for forcing frequency down sweep for the system with the activated absorber. The system displacement response is shown by curve 2 (data along DA′IC′B′B), for forcing frequency up sweep for the system with the activated absorber. The absorber displacement response is shown by curve 4 (data along FGG′E′H′H), for forcing frequency down sweep for the system with the activated absorber. The absorber displacement response is shown by curve 5 (data along HEE′G′F′F), for forcing frequency up sweep for the system with the activated absorber. As will be explained in the next paragraph, the unique superposition of the system displacement response curves (1, 2, 3, and 6) and the absorber displacement response curves (4 and 5), respectively, was done to show the interaction of the vibration absorber and primary structure.

In Figure 3, curves 1–3, and 6 show characteristic responses of a system without and with an effective vibration absorber. These responses are similar to those obtained by other authors studying the effectiveness of different vibration absorbers [6, 8, 24]. Curves 1–3, and 6 clearly show that, for the given structure parameters, the vibration absorber reduces the resonance peak amplitude experienced by the system. As shown by curve 5, discontinuities (jump phenomena) at EE′ and FF′ were observed in the absorber displacement during the up sweep. The jump phenomena are similar to that observed in [12, 17] in the study of non-linear systems. The absorber down sweep experimental response, curve 4, also exhibits jumps at the locations GG′ and HH′. The absorber paths following E′G′F′ (curve 5) and G′E′H′ (curve 4), which are non-zero absorber amplitudes, will be referred to as *stable response* curves of up sweep and down sweep respectively. Points A′ and C′ (system displacement response), and E′ and G′ (absorber displacement response) are important and will be defined as the *starting* and *end* points of the *absorption region* during the energy exchange between the modes. This energy exchange is akin to that observed by other researchers while studying non-linear coupled oscillators with two-mode interactions [23, 25, 26]. For the current study, it was observed that the maximum energy transfer occurred when the autoparametric condition was satisfied ($\omega_s = 2\omega_a$). From Figure 3, it is also evident that within the *absorption region* the amplitude of the system is lower for the case when the absorber is activated (two d.o.f.) than for the case when the absorber is locked (one d.o.f.). It is worthy to note that on comparing curves 6 and 3, between A′ and D′, and curves 1 and 2, between C′ and B′, no energy transfer occurs from the primary structure to the absorber. On the contrary, energy transfer is from the absorber to the primary structure. Therefore, in this study, the region between point A′ and jump D′D, and between point C′ and jump BB′ is referred to as the *non-absorption region.*

Figures 4 and 5 show the responses of the system (with and without an activated absorber) and the vibration absorber for a frequency ratio tuned at $\omega_a = 0{\cdot}5\omega_s \pm \Delta\omega_s$. In both the figures, the forcing frequency was swept up. As shown in Figure 4, where $\Delta = -0{\cdot}05$, autoparametric interaction occurred at 5·23 Hz, which is less than the resonance frequency of 5·78 Hz. On the other hand, in Figure 5, where $\Delta = +0{\cdot}05$, the autoparametric interaction occurred at 6·4 Hz, which is greater than the resonance frequency of 5·78 Hz. It is clear that both autoparametric interactions have no significance

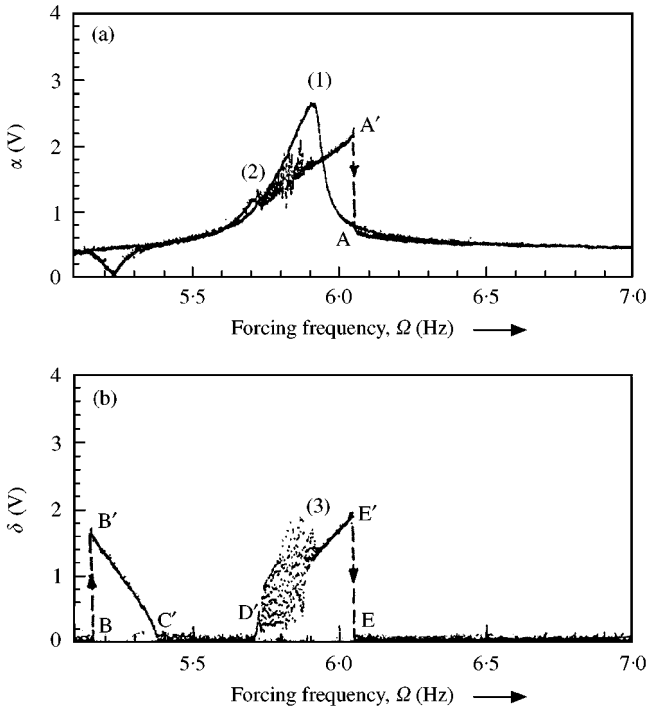

Figure 4. Experimental displacement response curves of $\omega_a = 0{\cdot}45\omega_s$ for up sweep: (a) system; (b) absorber. Response without activated absorber: (1) system. Response with activated absorber: (2) system; (3) absorber. Jump points. System: A and A′; absorber: B, B′, C′, D′, E and E′.

as they fall out of the *absorption region*. It is also apparent that the energy exchange, even in the neighborhood of the system resonance region at 5·78 Hz, is not as pronounced as observed in Figure 3. Although the maximum effect of the absorber occurred at the tuned frequency ratio of 0·5, the beneficial effect of the absorber persists over a very narrow frequency range. However, when frequency ratios are tuned for $\Delta = \pm 0{\cdot}05$, the absorber depicts a rather complex behavior. This is evidenced by the scatter of the response data between 5·7 and 5·9 Hz in Figure 4, and between 5·6 and 6·1 Hz in Figure 5. In order to obtain a better visualization of the response dynamics, the experiment was conducted over a smaller range of the forcing frequency. With the system parameter used in Figure 5, a narrow frequency sweep from 5·94 to 5·975 Hz was performed. The system and absorber displacement responses are shown in Figure 6. The displacement response of absorber clearly indicates that the response is periodic [Figure 6(a)]. The displacement response of the system is characterized by scattered data [Figure 6(b)]. A detailed experiment was performed at the forcing frequency of 5·965 Hz and the results are plotted in Figure 7. Figure 7 shows the reconstructed dynamics, time histories and FFT spectra for $\Omega = 5{\cdot}965$ Hz. The technique used to derive the reconstructed dynamics is the same as that used in reference [20]. Figure 7(a) is the phase diagram of the velocity response versus displacement response of the primary system. Figure 7(b) is the phase diagram of the displacement response of the primary system versus the displacement response of the absorber. This figure shows that there is a periodic interaction between the primary system and absorber. It should be added, though, that the figure does not conclusively reveal the type of periodic interaction. Figure 7(c) is the phase diagram of the velocity response versus displacement response of the absorber. Figure 7(d) and 7(e) is the time series and FFT of the

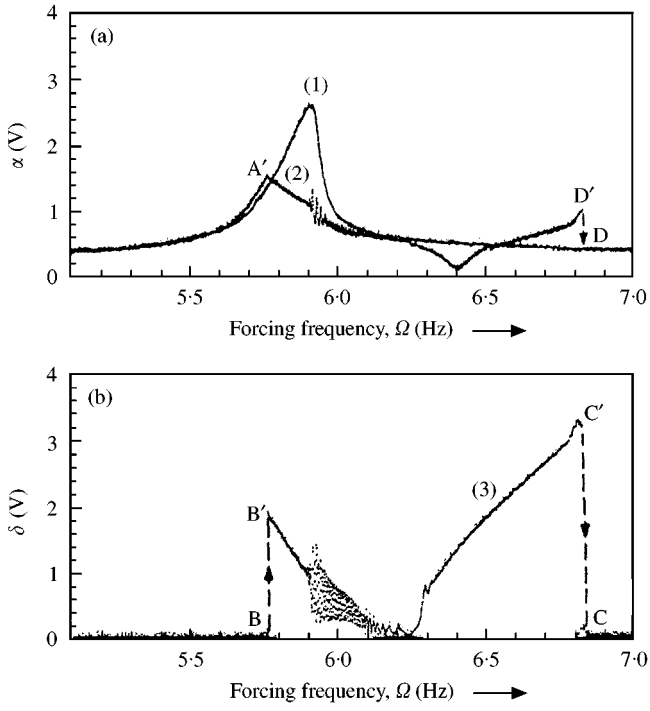

Figure 5. Experimental displacement response curves for $\omega_a = 0{\cdot}55\ \omega_s$ for up sweep: (a) system; (b) absorber. Response without activated absorber: (1) System. Response with activated absorber: (2) system; (3) absorber. Jump points. System: A′, D and D′; absorber: B, B′, C and C′.

primary system respectively. Figure 7(f) and 7(g) is the time series and FFT of the absorber, respectively. From Figure 7(a) through 7(g) it is clear that the response around 5·965 Hz is periodic with many harmonics involved in the response dynamics of both system and absorber. Hence, this displacement response can be characterized as quasi-periodic.

To determine the control parameters related to the *absorption region*, additional frequency sweep experiments were carried out. The results of these experiments, mapping the change in the absorption region with respect to the natural frequency of the system and forcing amplitude, are shown in Figure 8. To shed light on how the data points in Figure 8 were obtained, one has to refer back to Figure 3. In Figure 3, the system was adjusted to have a natural frequency of 5·78 Hz, and the forcing amplitude was set at 2·28 mm, and the resulting *absorption region* was the difference between the *starting* point A′ and the *end* point C′, specifically, 6·1–5·6 Hz = 0·5 Hz. According to this information, the natural frequency of 5·78 Hz is plotted against the *absorption region* of 0·5 Hz to yield point K in Figure 8. Similarly, the remaining 11 data points were extracted from the additional experiments, alluded to previously, to yield Figure 8. It is clear from this figure, that when the system is adjusted to have a high natural frequency, the *absorption region* expands. This figure also reveals that the *absorption region* is significantly increased when the system is exposed to a higher amplitude excitation. In summary, Figure 8 shows clearly that the control parameters related to the *absorption region* are the natural frequency of the system and the forcing amplitude.

Variations of the *absorption region* and *non-absorption region* with respect to the forcing amplitude for different mass ratios were also investigated. Results are illustrated in Figure 9(a) and 9(b). Referring to Figure 3, for which $f = 2{\cdot}28$ mm and $r_m = 0{\cdot}086$, the four

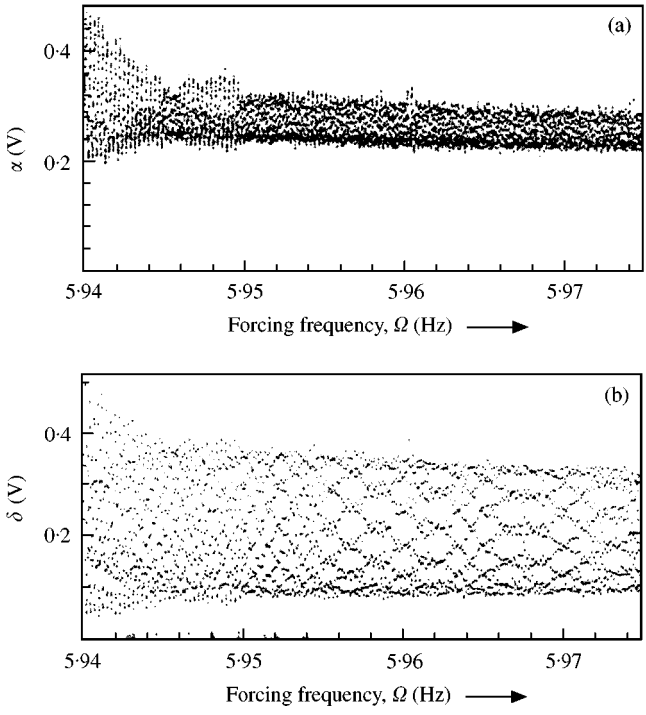

Figure 6. Expanded experimental displacement response curves for $\Omega \in (5{\cdot}94, 5{\cdot}975)$ Hz: (a) system; (b) absorber.

points D′A′C′B′ correspond to the four points 4123, respectively, in Figure 9(a). The additional data points were then obtained by varying the forcing amplitude, f, downward. It is observed that both regions change with respect to the forcing amplitude. A higher forcing amplitude translates into a larger range of the *absorption region*. Experiments similar to those performed to obtain Figure 9(a) were conducted to obtain Figure 9(b) for $r_m = 0{\cdot}267$. Both Figure 9(a) and 9(b) shows similar trends. To further investigate this similarity in the aforementioned trends, the mass ratio was varied for a fixed forcing amplitude $f = 2{\cdot}28$ mm. The results of this study are presented Figure 9(c). Again, referring to Figure 3, for which $f = 2{\cdot}28$ mm and $r_m = 0{\cdot}086$, the four points D′A′C′B′ correspond to the four points 4123, respectively, in Figure 9(c). Figure 9(c) confirms that the mass ratio has no effect on the absorption regions at a constant forcing amplitude. In passing, for experiments with a high forcing amplitude ($f = 2{\cdot}28$ mm) and high natural frequency ($\omega_s = 25{\cdot}0$ Hz) of the system, the authors observed that the absorber device succumbed to fatigue failure.

3.2. RANDOM EXCITATION

For all tests under random excitation, the natural frequency, ω_s, of the system was adjusted at 7·2 Hz. And for the initial set of experiments, the detuning ratio was $r_f = \omega_a/\omega_s = 0{\cdot}50$. Thus, the natural frequency of the absorber was tuned to 3·6 Hz. The system was designed such that by simply adjusting the length of the beam of the vibration absorber, the detuning ratio could be varied. For the random excitation, the automatic random vibration equalizer analyzer (ARVEA) was set to a spectral density of 0·011 g^2/Hz with a bandwidth from 3 to 21 Hz (Figure 10). This was done to excite the system in the

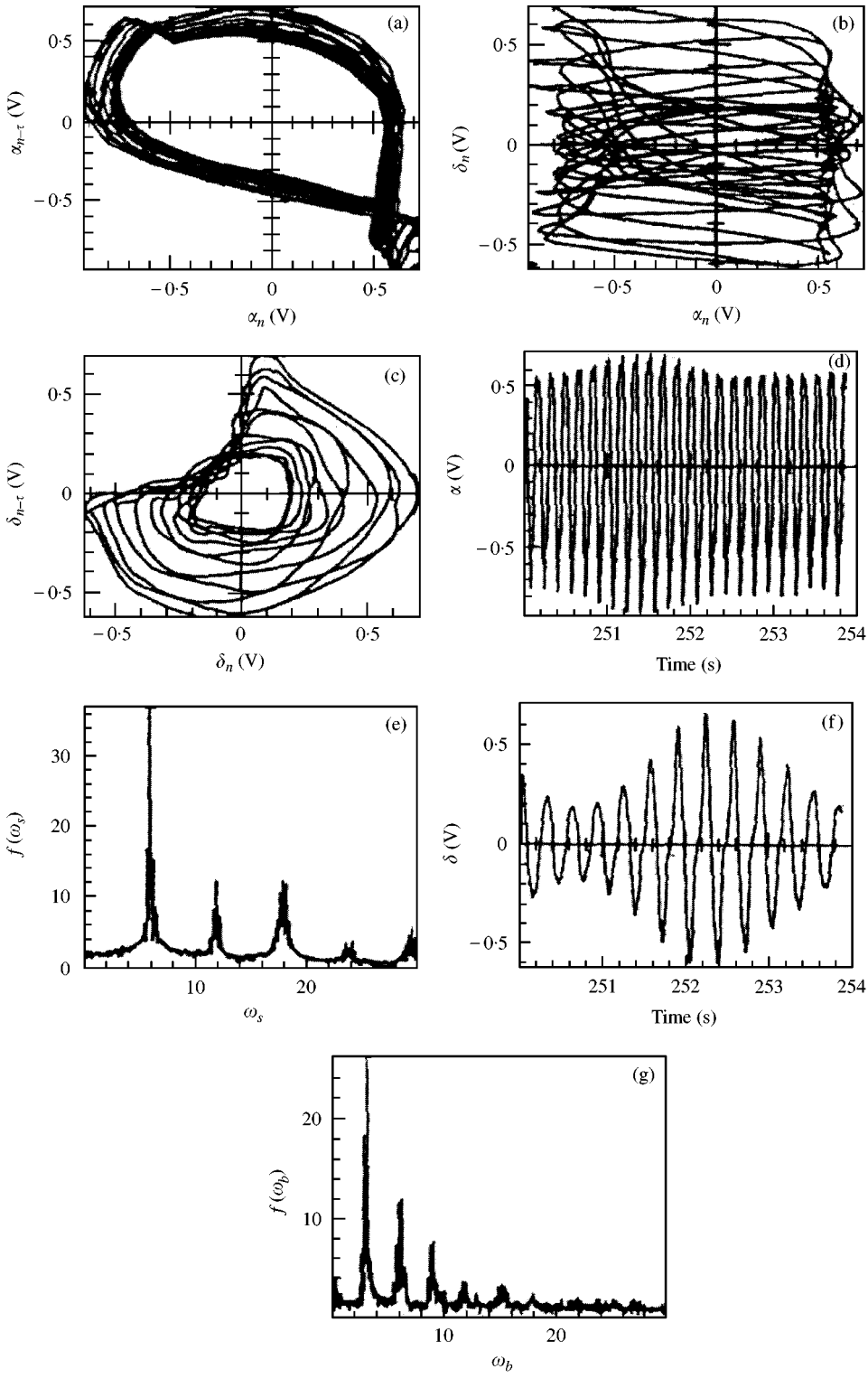

Figure 7. Detailed dynamics at the forcing frequency $\Omega = 5{\cdot}965$ Hz; (a), (b) and (c) phase diagrams; (d) oscillation in time domain; (e) FFT of (d); (f) oscillation in time domain; (g) FFT of (f).

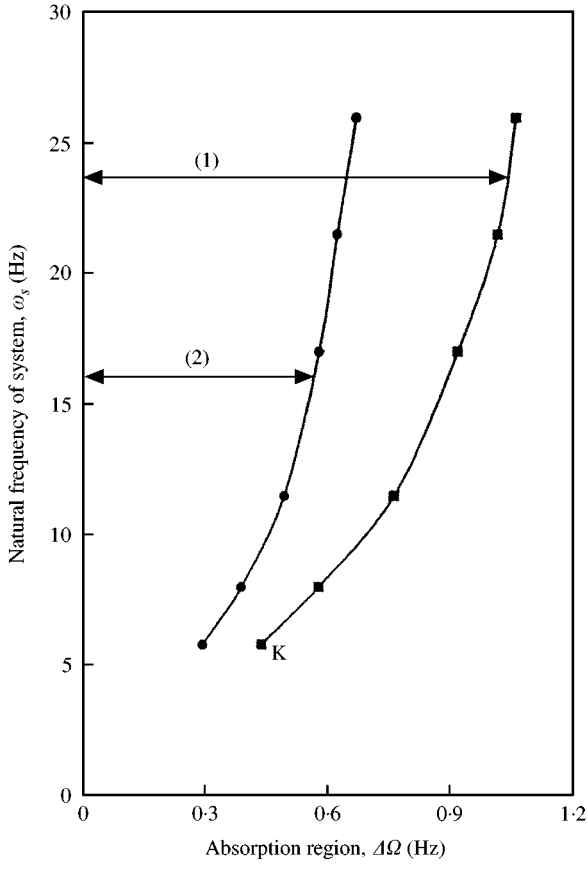

Figure 8. Variation of the absorption region with natural frequency of system, and forcing amplitude: (1) forcing amplitude 2·28 mm; (2) forcing amplitude 1·3 mm.

neighborhood of its fundamental natural frequency ($\omega_s = 7{\cdot}2$ Hz), while limiting the number of excited modes. The inclusion of higher than fundamental modes of vibration would have led to complex response motions of the system [22]. The up and down jumps on the spectral density level can be in part attributed to the coincidence of the spectral line with the borderline between the two frequency bands [27]. The other reason for the observed jumps was that it was difficult to exactly adjust the levels of the frequencies on the analog ARVEA. The sampling rate should be at least twice the maximum frequency of the measured system [28]. Therefore, for this study, a sampling rate of 100 Hz was chosen for each channel, which was sufficient for measuring the vibration of this system under random excitation containing the frequencies between 3 and 21 Hz.

Generally, stochastic experiments yield random data. Such time series are often studied by observing the system mean square response and power spectral density (PSD). The PSD is also referred to as the mean square spectral density. The PSD is a measure of the frequency content of the total process. It has also been shown that the response of a system and possible modal interaction can satisfactorily be investigated by studying the second moment of the response [29]. For this study, the second moment or mean square value of all data points, $\Psi^2(t_n)$, was calculated using [30]

$$\Psi^2(t_n) = \frac{1}{n}\sum_{i=1}^{n} X^2(t_i), \quad n = 1, 2, 3, \ldots, N, \tag{1}$$

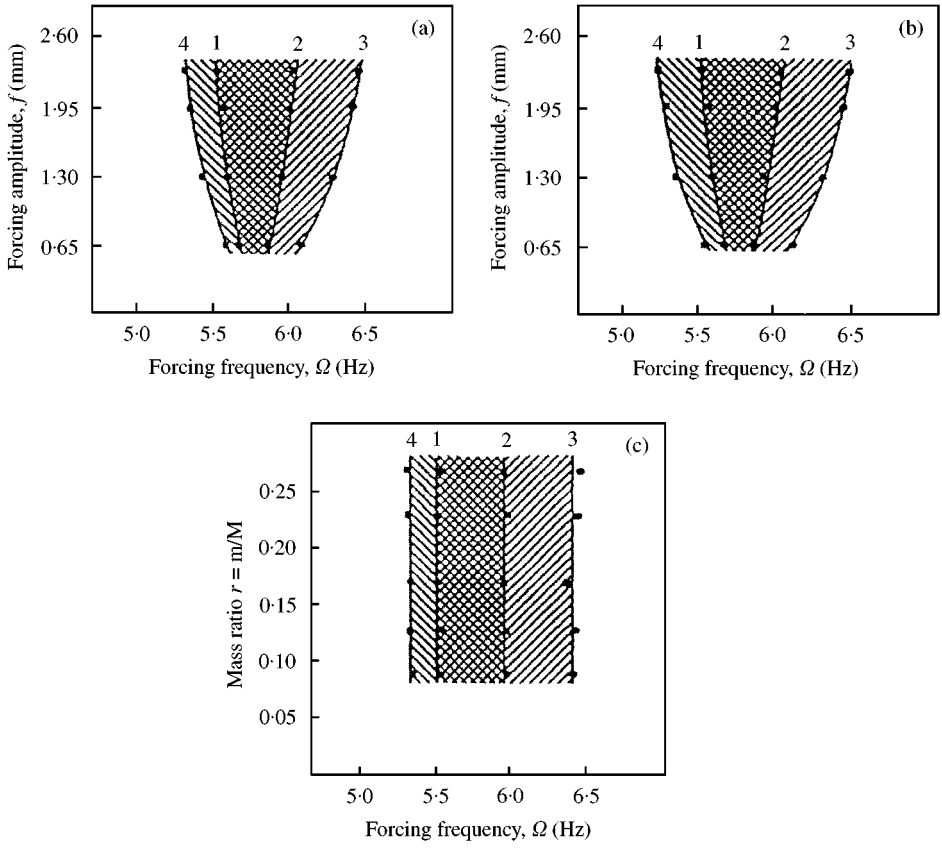

Figure 9. Absorption and non-absorption regions: (a) mass ratio $r_m = 0{\cdot}086$, (b) mass ratio $r_m = 0{\cdot}267$, and (c) forcing amplitude $f = 2{\cdot}28$ mm. Lines. Up sweep: 1, absorber started oscillation: 2, absorber stopped oscillation. Down sweep: 2, absorber started oscillation; 4, absorber stopped oscillation.

where $X(t_i)$ is the data signal and N is the total number of data points. But on the other hand, since the latter time series are not periodic, classical Fourier analysis cannot be used to obtain PSD directly from the time data [31]. Bendat and Piersol [30] note that there are three approaches in determining the PSD from experimental data, namely, filtering–squaring–averaging operations, finite Fourier transforms, and the autocorrelation function. The method based on the autocorrelation function uses the Wiener–Khintchine transform pair that calls for a Fourier cosine transform of the autocorrelation function [32]. This is the method used to obtain the frequency-domain characteristics of the system studied in this paper. Based on this methodology, for the ARVEA excitation setting of Figure 10, the shaker sample time history [Figure 11(a)], mean square response [Figure 11(b)], the autocorrelation function [Figure 10(c)], and the PSD (FFT of the autocorrelation function). Figure 11(d) are derived. The area under the PSD and the value of the autocorrelation at $\tau = 0$, are both approximately equal to the stationary mean square response $[E[\ddot{U}^2] = 0{\cdot}24\ V^2]$ [33]. It should also be noted that in Figure 11(d), the shaker acceleration response is true to the excitation signal (Figure 10) in that frequencies between 3 and 21 Hz are dominantly excited. This excitation level was used for all the experiments in this paper.

The spectral density functions for the displacement response of the system and vibration absorber are shown in Figure 12(a) and 12(b) respectively. The latter experiments were

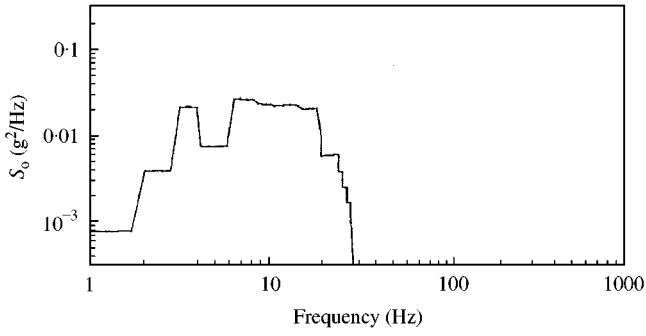

Figure 10. Power spectral density function of excitation signal.

conducted with a detuning ratio, $r_f = 0{\cdot}50$. It is evident from Figure 12(a) and 12(b) that both the system and absorber are excited about their respective natural frequencies, hence the single spike around the natural frequency. This implies that the responses of the system and absorber have strong periodic overtones. These results are in agreement with those obtained by Ibrahim *et al.* [23].

Figure 13(a) and 13(b) shows the mean square of the displacement response of the system, and absorber for a detuning ratio, r_f, of 0·50 and a mass ratio, r_m, of 0·165 respectively. The trends of the mean square responses are in agreement with those observed by Ibrahim *et al.* [23]. Figure 13 [and Figure 11(b)] shows that the system and absorber (and shaker) signals can be assumed to be stationary after approximately 800 s. However, it was observed that for detuning ratios lesser than or greater than 0·50 the mean square curve reaches stationary values at different times. After carrying out a series of experiments, in this study, for all the experiments performed for different detuning parameters, stationarity was taken to occur after 1600 s.

To investigate the effect of the detuning ratio on the autoparametric interaction a set of experiments were conducted in the neighborhood of the detuning ratio of $r_f = 0{\cdot}50$. Results of these experiments are represented in Figure 14. From this figure, it is clear that strong autoparametric interaction between the main mass and the absorber occurred in the neighborhood of $r_f = \omega_a/\omega_s = 0{\cdot}50$. This is evidenced by the highest absorber and the lowest system stationary mean square responses occurring at about $r_f = 0{\cdot}50$. This is in line with what Ibrahim *et al.* [23] observed in similar studies. Nayfeh and Serhan [26], while studying a different system also observed similar energy exchange similar to the autoparametric resonance. As can be seen in Figure 14, the observed stationary values are scattered. In part, this can be attributed to the following: (1) difficulties in performing all tests at exactly the same excitation level (i.e., human errors) [34]; (2) possibility of getting incompatible data from the sensors and/or instruments (noise, the loss of the accuracy and sensitivity of the sensors in time, etc.); and (3) fatigue failure of steel spring beam (i.e., when the steel spring beam is changed it is difficult to locate the piezo films at the same location, which may affect the voltage output reading of the sensor).

To investigate the dependence of the mean square responses on the mass ratio of the absorber to primary structure, r_m, a set of experiments were conducted for varying mass ratios. For all these tests, the mass ratio is adjusted by changing the mass of the absorber while keeping that of the primary structure fixed. It should be noted that in this set of experiments, the detuning ratio was kept constant at $r_f = 0{\cdot}50$, thus varying r_m does directly relate to varying r_f. While adjusting the mass ratio, the detuning ratio was kept constant by

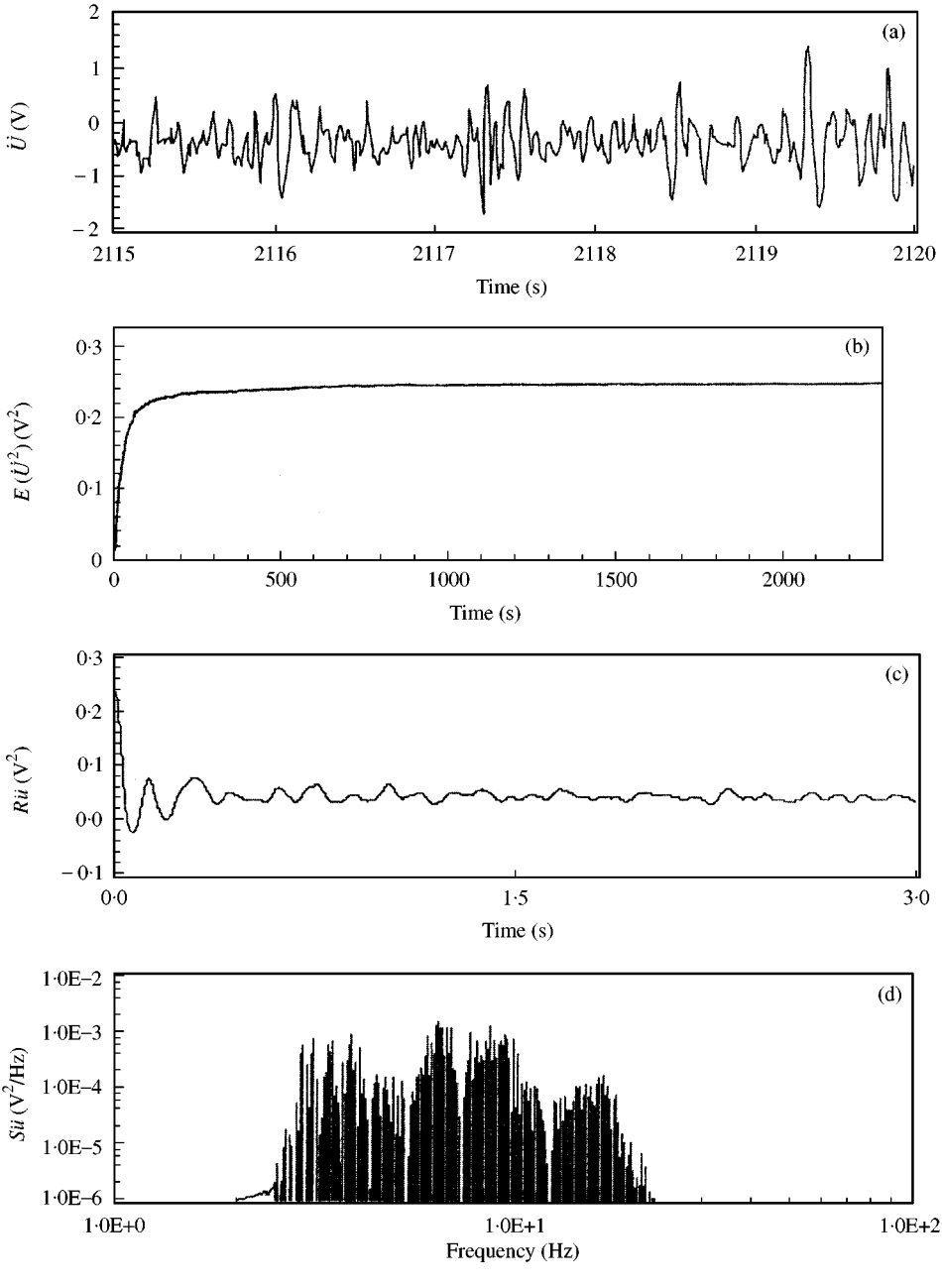

Figure 11. Shaker characteristics ($r_f = 0{\cdot}50$): (a) sample time history, (b) mean square response, (c) autocorrelation function, and (d) power spectral density.

simply adjusting the length of the beam of the absorber. The extracted stationary mean square responses are shown in Figure 15(a) and 15(b). Figure 15(a) shows that by increasing the mass ratio the stationary mean square response of the system decreases. However, it is interesting to note that the mean square response of the absorber remains approximately the same [Figure 15(b)].

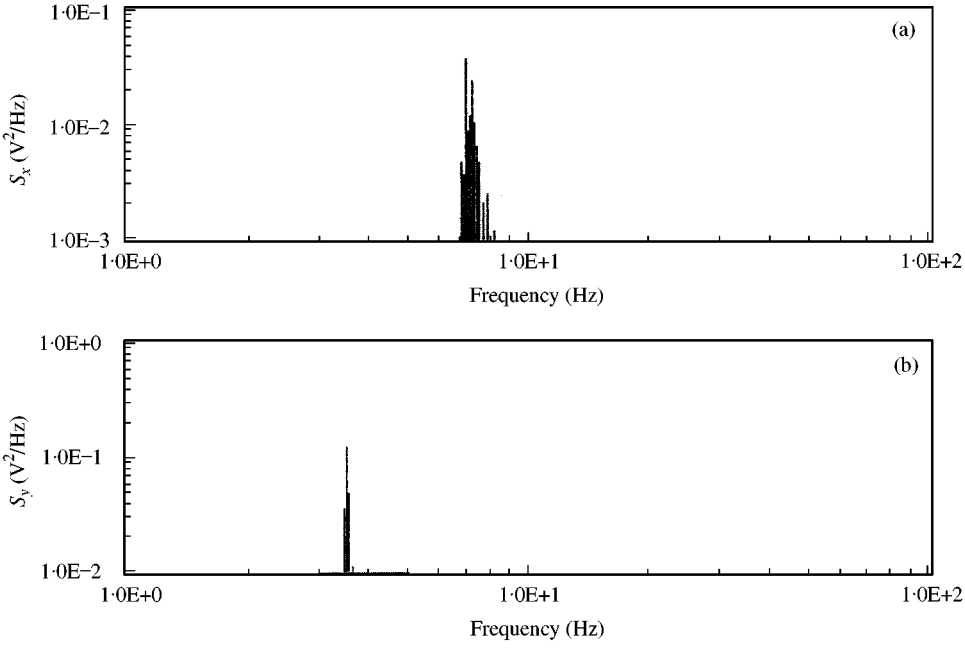

Figure 12. Power spectral density function of the displacement response ($r_f = 0{\cdot}50$): (a) system, and (b) absorber.

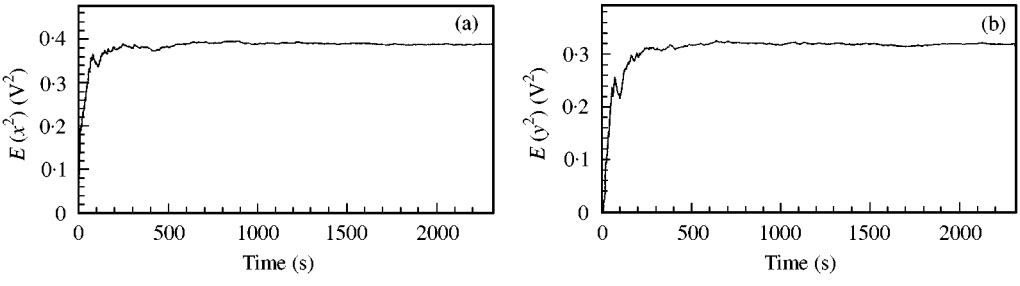

Figure 13. Mean squares of the displacement response ($r_f = 0{\cdot}50$): (a) system, and (b) absorber.

4. CONCLUSIONS

This paper presents a comprehensive experimental study of the effectiveness of a passive vibration absorber applied to a primary structure simulating a one-story building under sinusoidal and random excitations. The vibration absorber and primary structure constituted a system with an autoparametric coupling.

For the sinusoidal excitation, and *absorption region* for the absorber was defined. To determine the control parameters related to the *absorption region*, frequency-sweep experiments were conducted. Consequently, the effects of the forcing frequency, forcing amplitude, mass ratio and detuning ratios on the *absorption region* were established. Results of the study indicated that a considerable energy exchange occurs between the primary

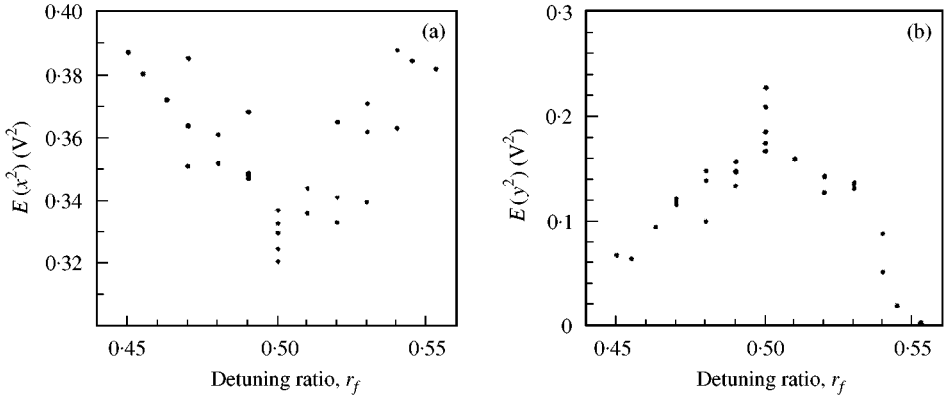

Figure 14. Dependence of the mean square of the displacement responses on the frequency or detuning ratio: (a) system, and (b) absorber.

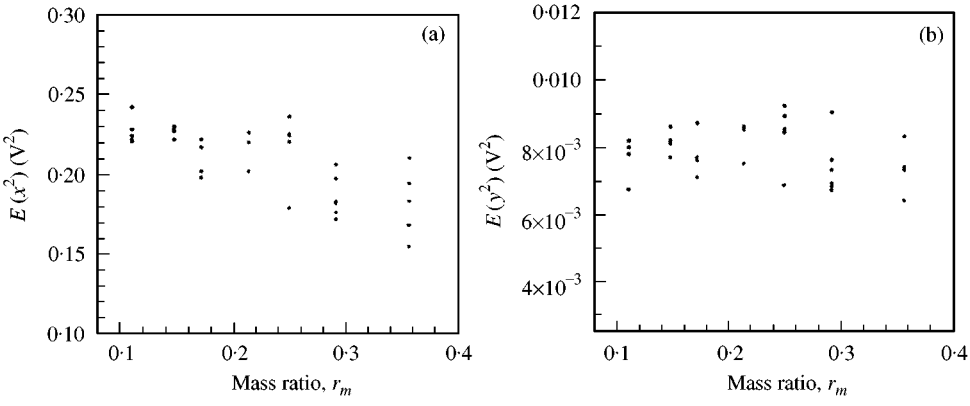

Figure 15. Dependence of the mean square of the displacement responses on the mass ratio: (a) system, and (b) absorber.

structure and the absorber when the external resonance condition of $\Omega = \omega_s$ and the primary resonance condition of $\omega_a = 0{\cdot}5\omega_s$, are satisfied. However, the beneficial effect of the absorber persists over a very narrow frequency range. When frequency ratios are tuned to $\omega_a = 0{\cdot}45\omega_s$ and $\omega_a = 0{\cdot}55\omega_s$ the absorber showed an interesting response called the webs of periodic windows. But it was observed in both cases, that the autoparametric interactions have no significance as they fall out of the *absorption region.* Additional experiments also showed that higher forcing amplitude translates into a larger range of the *absorption region.* It was also shown that the effect of the mass ratio on the absorption region was insignificant. At an excitation frequency of 5·965 Hz it was shown that the displacement response was quasi-periodic.

For random excitation, the interactions of the absorber and primary structure were studied based on the *stationary* mean square responses. Strong autoparametric interaction between the primary structure and the absorber occurred in the neighborhood of $r_f = \omega_a/\omega_s = 0{\cdot}50$. This is in agreement with results obtained by other researchers. On increasing the mass ratio, the stationary mean square response of the system decreased, while that of the absorber remains approximately the same.

REFERENCES

1. J. Q. Sun, M. R. Jolly and M. A. Norris 1995 *Journal of Mechanical Design* **117**, 234–242. Passive, adaptive and active tuned vibration absorbers—a survey.
2. I. N. Jordanov and B. I. Cheshankov 1988 *Journal of Sound and Vibration* **123**, 157–170. Optimal design of linear and non-linear dynamic vibration absorbers.
3. Y. L. Xu, K. C. S. Kwok and B. Samali 1990 *Research Report* R617, *Department of Civil and Mining Engineering, University of Sydney*. Control of wind-induced vibration by tuned mass dampers.
4. P. Watts 1883 *Transactions of the Institution of Naval Architects* **24**, 90–165. On a method of reducing the rolling of ships at sea.
5. J. Ormandroyd and J. P. Den Hartog 1928 *Transaction of American Society of Mechanical Engineering* **50**, A9–A22. The theory of dynamic vibration absorber.
6. T. Dahlberg 1989 *Journal of Sound and Vibration* **132**, 518–522. On optimal use of the mass of dynamic vibration absorber.
7. K. Kawazoe, I. Kono, T. Aida, T. Aso and K. Ebisuda 1998 *Journal of Engineering Mechanics* **124**, 476–479. Beam-type dynamic vibration absorber comprised of free–free beam.
8. P. A. Hitchcock, K. C. S. Kwok, R. D. Watkins and B. Samali 1997 *Engineering Structures* **19**, 135–144. Characteristics of liquid column vibration absorbers (LCVA)—II.
9. V. J. Modi and M. L. Seto 1998 *Journal of Vibration and Control* **4**, 381–404. Passive control of flow-induced oscillations using rectangular nutation dampers.
10. P. H. Wirsching and G. W. Campbell 1974 *Earthquake Engineering and Structural Dynamics* **2**, 303–312. Minimal structural response under random excitation using the vibration absorber.
11. R. A. Ibrahim and A. D. Barr 1975 *Journal of Sound and Vibration* **42**, 159–179. Autoparametric resonance in a structure containing liquid. Part 1: two mode interaction.
12. A. H. Nayfeh and D. T. Mook 1979 *Nonlinear Oscillations*. New York: Wiley.
13. E. Sevin 1961 *Journal of Applied Mechanics* **28**, 330–334. On the parametric excitation of pendulum-type vibration absorber.
14. J. Shaw, S. W. Shaw and A. G. Haddow 1989 *International Journal of Non-Linear Mechanics* **24**, 281–293. On the response of the non-linear vibration absorber.
15. F. R. Arnold 1955 *Journal of Applied Mechanics* **22**, 487–492. Steady-state behavior of system provided with nonlinear dynamic vibration absorber.
16. O. Cuvalci, B. Gumus and A. Ertas 1996 *Proceedings of the World Conference on Integrated Design and Process Technology* **3**, 391–398. An experimental investigation of nonlinear system in autoparametric region.
17. O Cuvalci and A. Ertas 1996 *Journal of Vibration and Acoustics* **118**, 558–566. Pendulum as vibration absorber for flexible structures: experiments and theory.
18. A. G Haddow, A. D. S. Barr and D. T. Mook 1984 *Journal of Sound and Vibration* **97**, 451–473. Theoretical and experimental study of model interaction in a two-degree-of-freedom structure.
19. S. F. Masri and T. K. Caughey 1966 *Journal of Applied Mechanics* **88**, 586–592. On the stability of the impact damper.
20. G. Mustafa and A. Ertas 1995 *Journal of Sound and Vibration* **182**, 393–413. Dynamics and bifurcations of a coupled column-pendulum oscillator.
21. A. H. Nayfeh and L. D. Zavodney 1986 *Journal of Sound and Vibration* **107**, 329–350. The response of two-degree-of-freedom system with quadratic non-linearities to a combination parametric resonance.
22. J. W. Roberts 1980 *Journal of Sound and Vibration* **69**, 101–116. Random excitation of a vibratory system with autoparametric interaction.
23. R. A. Ibrahim, Y. J. Yoon and M. G. Evans 1990 *Nonlinear Dynamics* **1**, 91–116. Random excitation of nonlinear coupled oscillation.
24. A. Ertas, O. Cuvalci and S. Ekwaro-Osire 1998 *Conference on Nonlinear Vibrations, Stability, and Dynamics of Structures and Mechanisms Proceedings, VPI&SU, Blacksburg, VA*. Dynamics of a flexible structure with pendulum studied at various angles between vertical and the horizontal positions.
25. R. S. Haxton and A. D. S. Barr 1972 *Journal of Engineering for Industry* **94**, 119–125. The autoparametric vibration absorber.
26. A. H. Nayfeh and S. J. Serhan 1991 *Journal of Sound and Vibration* **151**, 291–310. Response moments of dynamic systems with modal interactions.
27. J. D. Smith 1989 *Vibration Measurement and Analysis*. London: Butterworth.
28. S. Goldman 1991 *Vibration Spectrum Analysis*. New York: Industrial Press.

29. L. D. LUTES and S. SARKANI 1997 *Stochastic Analysis of Structural and Mechanical Vibrations*. Upper Saddle River, NJ: Prentice-Hall.
30. J. S. BENDAT and A. G. PIERSOL 1986 *Random Data, Analysis and Measurement Procedures*. New York: Wiley.
31. D. E. NEWLAND 1993 *An Introduction to Random Vibrations, Spectral and Wavelet Analysis*. London: Longman; third edition.
32. D. G. CHILDERS 1997 *Probability and Random Processes*. New York: McGraw-Hill.
33. K. G. MCCONNELL 1995 *Vibration Testing: Theory and Practice*. New York: Wiley.
34. R. A. IBRAHIM 1991 *Applied Mechanics Review* **44**, 423–446. Nonlinear random vibration: experimental results.

APPENDIX A: NOMENCLATURE

$E[\bullet^2]$	mean square value of $\bullet$
f	forcing amplitude (peak-to-peak)
M	mass of primary structure
m	mass of vibration absorber
r_f	detuning (frequency) ratio, ω_a/ω_s
r_m	mass ratio of the absorber to primary structure, m/M
$R_{(\bullet)}(\tau)$	autocorrelation of $\bullet$
$S_{(\bullet)}(\omega)$	power spectral density (PSD) function of $\bullet$
V	volts
$\ddot{U}$	acceleration response of shaker
x	displacement response of system
y	displacement response of absorber
α	displacement response of system
δ	displacement response of absorber
ω_a	natural frequency of the absorber
ω_s	natural frequency of the system (with absorber locked)
$\Delta\Omega$	forcing frequency difference
$\Psi^2(t_n)$	mean square (second moment) of the acquired data
Ω	forcing frequency